Thioaluminogermanate $M(AlS_2)(GeS_2)_4$ (M = Na, Ag, Cu): Synthesis, Crystal Structures, Characterization, Ion-Exchange and Solid-State ^{27}Al and ^{23}Na NMR Spectroscopy

Fatimah Alahmari,[*,†,‖] Bambar Davaasuren,[†,¶] Abdul-Hamid Emwas[‡] and Alexander Rothenberger[†]

[*] Corresponding author: fatimah.alahmary@kaust.edu.sa

[†] Physical Science and Engineering Division, [‡] Core Labs, King Abdullah University of Science and Technology (KAUST), Thuwal 23955-6900, Kingdom of Saudi Arabia

[‖] Institute for Research and Medical Consultations (IRMC), Imam Abdulrahman bin Faisal University, Dammam 31441, Kingdom of Saudi Arabia

[¶] *Current affiliation*: Institute for Energy and Climate Research, Materials Synthesis and Processing (IEK-1), Forschungszentrum Jülich GmbH, 52425 Jülich, Germany

Keywords: Thioaluminogermanate; Ion-exchange; Al NMR; Na NMR; Chalcogenides

Abstract

The new thioaluminogermanate $Na(AlS_2)(GeS_2)_4$ (**1**) was successfully synthesized by direct combination reaction. The compound crystallizes in the monoclinic space group $P2_1/n$ (no. 14) with unit cell parameters a = 6.803(3) Å, b = 38.207(2) Å, c = 6.947(4) Å, β = 119.17(3)°. The crystal structure is composed of a $[(AlS_2)(GeS_2)_4]^{1-}$ 3D polyanionic network, in which Al and Ge atoms share the atomic positions, and Na cations are occupying the channels and voids formed by the connection of $(Ge/Al)S_4$ tetrahedra. The title compound shows cation-exchange property with monovalent Ag^+ and Cu^+ ions, at room temperature in solvent media, resulting in the formation of the isostructural compounds $Ag(AlS_2)(GeS_2)_4$ (**2**) and $Cu(AlS_2)(GeS_2)_4$ (**3**), respectively. The ion-exchange products $Ag(AlS_2)(GeS_2)_4$ (**2**) and $Cu(AlS_2)(GeS_2)_4$ (**3**) show higher air stability and narrower bandgap energies compared to the parent compound $Na(AlS_2)(GeS_2)_4$ (**1**).

Introduction

The coordination and synthetic chemistry of chalcogenogermanates is extensively studied.[1-3] The formation of different anionic partial structures by linking of basic building units $[Ge_xQ_y]^{n-}$ (Q = S, Se or Te) makes them interesting from the structural point of view.[4-6] In the case of thiogermanates, the compositional and structural flexibility are revealed by the formation of various building blocks constructed from GeS_4 tetrahedra connected in different manners.[1] For example, $[GeS_4]^{4-}$ isolated tetrahedra, $[GeS_3]^{2-}$ chains, $[Ge_2S_6]^{4-}$ dimers, $[Ge_2S_6]^{6-}$ ethane-like dimers, $[Ge_2S_7]^{6-}$ fragments and $[Ge_4S_{10}]^{4-}$ adamantane-like units are found in thiogermanates.[7] Many of these compounds feature interesting physical and chemical properties and have found application in different areas. For instance, $Cs_4Pb_4Ge_5S_{16}$ has been used as cathodoluminescent,[8] $Li_2Ga_2GeS_6$ shows second-harmonic generation (SHG) response,[9] Cu_2ZnGeS_4 demonstrates photocatalytic activity for H_2 evolution,[10] and the recently reported high surface area porous MAu_2GeS_4-chalcogel (M = Co, Ni) heterogeneous hydroamination catalysts prepared from $K_2Au_2GeS_4$.[11]

The structural chemistry of chalcogenogermanates was successfully extended to the aluminosilicate relatives (zeolite-like chalcogenides),[12] by the insertion of Al^{3+} cations into the chalcogenogermanate framework. The similarity between the ionic radii of Al^{3+} and Ge^{4+} explains the possibility of the homogeneous distribution of Al within the chalcogenogermanate framework to build up negatively charged $[Al_xGe_{1-x}Q_4]^{x-}$ tetrahedra.[13] The *A*/Al/Ge/S (*A* = alkali metal, transition metal) family remains largely unexplored and only two structures are reported up to date, $Rb_3(AlQ_2)_3(GeQ_2)_7$ (*Q* = S, Se),[12] and $A(AlS_2)(GeS_2)$ (*A* = Na, K).[14] The thiogermanates were mainly synthesized by conventional solid state and hydro(solvo)thermal synthetic routes.[15-18] One of the most powerful methods is the reactive molten alkali metal polysulfide flux, which has been employed in the exploratory synthesis of a large set of ternary and quaternary thiogermanates.[8, 19] The advantage of using alkali metals is primarily due to their reactivity with sulfur at lower temperatures and their influence on the dimensionality and the crystallinity of the subject compounds.[20]

Due to their rich compositional diversity, broad structural flexibility and soft S^{2-} ligands, the metal sulfides attracted considerable attention as ion-exchange materials for industrial and environmental applications. The soft S^{2-} ligand leads to a high selectivity toward soft or relatively soft metal ions in the ion-exchange process.[21-22] Demand-driven state-of-the-art research projects are carried out to synthesize different metal sulfides for capturing of radionuclides from nuclear waste and decontamination of water solutions from various heavy metal ions.[23-25] For example, $(Me_2NH_2)_{1.33}(Me_3NH)_{0.67}Sn_3S_7 \cdot 1.25H_2O$ acts as an efficient ion-exchanger for rare earth metals recovery,[21] $K_{2x}M_xSn_{3-x}S_6$ (M = Mn^{2+}, KMS-1; M = Mg^{2+}, KMS-2; *x* = 0.5 to 1) show superior ion-exchange properties toward cations related to nuclear waste (such as Cs^+, Sr^{2+}, Ni^{2+} and UO_2^{2+}), and heavy metal ions from aqueous wastes (such as Hg^{2+}, Pb^{2+}, Cd^{2+}).[22]

Herein, we report on the synthesis and characterization of a new thioaluminogermanate $Na(AlS_2)(GeS_2)_4$ (**1**). The compound **1** shows a unique ion-exchange property in solvent media, at room temperature, toward the monovalent transition metals (Ag and Cu). As a result, isostructural compounds $Ag(AlS_2)(GeS_2)_4$ (**2**) and $Cu(AlS_2)(GeS_2)_4$ (**3**) have been obtained. The coordination of Al atoms in these compounds has been investigated by the solid-state ^{27}Al NMR, while the replacement of the Na^+ ions with Ag^+ or Cu^+ ions was examined by ^{23}Na NMR spectroscopy.

Experimental Section

All sample preparations and handling were carried out in an N_2-filled glovebox. The starting materials S (99.99%, Alfa Aesar), Al (Alfa Aesar 99.5 %), Ge (Sigma Aldrich 99.99%), $AgNO_3$ (Sigma Aldrich 99.99%), and $CuCH_3COO$ (Sigma Aldrich 99.99%) were used as received. Na_2S was prepared by liquid ammonia reaction according to a reported procedure.[26]

Synthesis of $Na(AlS_2)(GeS_2)_4$ (1)

$Na(AlS_2)(GeS_2)_4$ (**1**) was prepared by direct combination reaction of Na_2S (0.37 mmol), Al (0.75 mmol), Ge (3.02mmol) and elemental S (7.18 mmol). The mixture was filled and hand-pressed into a glassy carbon crucible, which was placed into a silica tube and flame-sealed under vacuum. Phase pure yellowish-orange crystalline material was obtained after heating the sample at 850 °C for 72 hours followed by slow cooling down to 400 °C with 2 °C/h rate, before cooling down to room temperature. Compound **1** partially decomposes after exposure to air for one week, and does not dissolve in some organic solvents such as N,N-Dimethylformamide (DMF), methanol, ethanol, acetone, and diethyl ether.

Ion-exchange reactions

The ion-exchange reactions were carried out at room temperature in 20 mL glass vials. The molar ratio of the compound **1** and the Ag- or Cu-salts was taken as 1:1. $Ag(AlS_2)(GeS_2)_4$ (**2**) and $Cu(AlS_2)(GeS_2)_4$ (**3**) were prepared by ion-exchange reaction of **1** with $AgNO_3$ and $CuCH_3COO$, respectively. 50 mg of **1** was added to a solution of 12.8 mg $AgNO_3$ (or 9.3 mg $CuCH_3COO$) in 3 mL extra dry DMF. The mixture was slowly stirred for three days to ensure the completeness of the ion-exchange reaction. Homogeneous ion-exchange products were isolated in the form of dark grey (**2**) and light brown (**3**) block-shaped crystals after washing the reaction products with DMF and drying with diethyl ether. $Ag(AlS_2)(GeS_2)_4$ (**2**) also can be prepared in acetonitrile solution using $AgNO_3$ or AgCl, while $Cu(AlS_2)(GeS_2)_4$ (**3**) can be obtained from acetonitrile, DMF and ethanol solutions using $CuCH_3COO$ or CuBr. Compound **2** and **3** are air-stable and do not dissolve in some organic solvents such as DMF, methanol, ethanol, acetone, and diethyl ether.

Characterization

The powder X-ray diffraction patterns were recorded using a STOE STADI MP X-ray diffractometer equipped with monochromatic Cu-*K*α1 (λ = 1.5406 Å) radiation and a DECTRIS MYTHEN 1K micro strip solid-state detector. The sample was prepared in acetate foils and mounted on the transmission sample holder. The ($2\theta + \omega$) scan type in the $10° < 2\theta < 90°$ range, with a scan step of 0.78° and 15 sec/step exposure time, was used for the measurements. The diffractometer was calibrated with NIST-Si standard prior to the measurements.

The single crystals were mounted on a glass fiber using perfluoroalkylether (viscosity 1800, ABCR GmbH & Co. KG, Karlsruhe, Germany). The samples were probed with a STOE IPDS 2 Single-Crystal X-ray Diffractometer, equipped with graphite monochromatized Mo-*K*α (λ = 0.71073 Å) radiation, at 200 K for compounds **1** and **2** and 150 K for **3**. The *X-Area* and *X-Shape* programs were used for data collection, determination, and refinement of the lattice parameters as well as for data reduction including LP correction.[27-28] The crystal structure was solved by direct methods and refined using

SHELXS2015 and SHELXL2015 program packages.[29] The graphical images of the crystal structure were produced using the program Diamond.[30]

Semi-quantitative elemental analyses were carried out with an FEI environmental scanning electron microscope ESEM Quanta 600 FEG – equipped with an EDX detector.

The solid-state ^{27}Al NMR and ^{23}Na NMR spectra were recorded on a Bruker 400 MHz AVANCE III NMR spectrometer equipped with 4 mm Bruker MAS probe (Bruker BioSpin, Rheinstetten, Germany). Each sample was packed evenly into 4 mm zirconia rotor and sealed at the open end with a Vespel cap. All spectra were recorded with 14 kHz spinning rate using one-pulse program with recycle delay time of 2 sec. Before the acquisition, the ^{27}Al chemical shift was referenced to 0.0 ppm using $AlCl_3(H_2O)_6$ and the ^{23}Na NMR spectra were referenced to 0.0 ppm using NaCl as an external reference. All spectra were then visually phased, and the baselines were adjusted manually. Bruker Topspin 3.5pl7 software (Bruker BioSpin, Rheinstetten, Germany) was used in all NMR experiments to record the spectra and to analyze the data.

Raman spectra were recorded with a HORIBA Jobin Yvon ARAMIS Raman spectrometer using the He-Ne-laser (473 nm) with a resolution of 50 cm^{-1}. The instrument was calibrated using the silicon standard at two different resolutions (10 cm^{-1} and 100 cm^{-1}), before the measurement.

UV-Vis. diffuse reflectance measurements were carried out at room temperature with a Varian UV-Vis-NIR Cary 5000 double beam, double monochromator spectrophotometer using the praying mantis accessories for solid samples. For the compounds **1** and **3**, measurements were done in the range 200-800 nm, while **2** was measured in the 200-2000 nm range, with a scan rate of 200 nm/min for all. KBr was used for the baseline correction.

Results and Discussion

Single crystals of **1**-**3** with appropriate sizes were isolated manually for single crystal analyses. Relevant crystallographic data and further details on data collection and structure refinements for **1**-**3** are summarized in Table 1. Energy-Dispersive X-ray (EDX) analysis on selected crystals, confirmed the presence of the elements in the atomic ratios of 1:1:4:10 (*M*:Al:Ge:S) where *M* is Na for **1**, Ag for **2** and Cu for **3** (Figure S1(Supporting Information SI)). EDX results were in a good agreement with crystal structure refinement results. The observed and calculated powder XRD patterns of all compounds are displayed in Figure S2 (SI). The powder XRD patterns of the compounds before and after exposure to air for a week are shown in Figure S3 (SI).

The atomic coordinates, site occupancy factors, and equivalent atomic displacement parameters of the atoms in compounds **1**, **2**, and **3** are given in Tables S1, S3, and S5, respectively (SI). Anisotropic atomic displacement parameters of the atoms for all compounds are listed in Tables S2, S4, and S6 (SI).

$Na(AlS_2)(GeS_2)_4$ (**1**), $Cu(AlS_2)(GeS_2)_4$ (**2**) and $Ag(AlS_2)(GeS_2)_4$ (**3**) are all isostructural. Therefore, the crystal chemistry will be discussed in details only for $Na(AlS_2)(GeS_2)_4$ (**1**).

Crystal Chemistry

$Na(AlS_2)(GeS_2)_4$ (**1**) crystallizes in the monoclinic space group $P2_1/n$ (no. 14). The crystal structure displays $[(AlS_2)(GeS_2)_4]^{1-}$ 3D polyanionic network, in which Al and Ge atoms share the atomic positions. The overall negative charge of the polyanionic framework is defined by the number of Al^{+3} forming negatively charged $(Al^{3+}(S_2)^{4-})^{1-}$ unit, as the $(Ge^{4+}(S_2)^{4-})$ unit is neutral. The Al/Ge mixed positions are four-fold coordinated by S atoms forming slightly distorted tetrahedral $(Ge/Al)S_4$ building blocks with average (Al/Ge)–S interatomic distances of d(Al/Ge–S) = 2.21 Å and average S–(Al/Ge)–S angles of 109.4 ° (Figure 1). This type of Al and Ge coordination is well-known and observed in all known ternary alkali thioaluminates,[31] and thiogermanates.[32-34] The condensation of the $(Ge/Al)S_4$ tetrahedral units (corner and edge-sharing) results in the 3D polyanionic arrangement, accommodating Na cations within the different channels. There are two different positions of Na atoms, Na1 and Na2 (Figure 1). Along *a* axis, Na1 and Na2 located in the biggest channels consisting of 20 connected tetrahedra (12 edge-shared and 8 corner-shared units) (Figure 2a). These channels are similar to the ones found in $Rb_3(AlS_2)_3(GeS_2)_7$.[12] Along *c* axis, only Na2 atoms occupy the parallelogram voids resulting from 6 edge shared tetrahedra (Figure 2b). Along the [101] direction, Na2 atoms occupy the voids resulting from 8 connected tetrahedra (4 edge-shared and 4 corner-shared units), while Na1 atoms occupy the voids resulting from 6 edge-shared tetrahedra (Figure 2c). The charge compensation and the distribution of the Na atoms within the negatively charged 6, 8, and 20 membered large channels explain the disorder and the rather big atomic displacement parameters of the Na atoms. The Na1 atom is coordinated by five S atoms forming distorted trigonal bipyramids, whereas the Na2 atom is coordinated by six S atoms forming a heavily distorted octahedron. The $(Na2)S_6$ octahedra are connected to each other in an edge-shared fashion forming chains running along *c*, which are connected to the individual $(Na1)S_5$ trigonal bipyramids via corner-sharing (Figure 2d). The average Na–S distance of 2.93 Å is in the same range with those observed in $NaAlP_2S_6$,[35] $Na_8Ge_4Pb_2S_{12}$ and $Na_8Ge_4Pb_2S_{12}$.[7]

The 3D polyanionic partial structure $[(AlS_2)(GeS_2)_4]^{1-}$ seems to be very rigid as no anionic lattice distortion was observed after the ion-exchange of $Na(AlS_2)(GeS_2)_4$ (**1**) with Ag^+ and Cu^+ cations. However, the cationic partial structure of **2** and **3** are rather heavily disordered compared to the parent compound **1**. As mentioned above, in compound **1** the Na atoms are distributed over two crystallographic positions. In the case of ion-exchanged compounds **2** and **3** the Ag and Cu cations are distributed over five and six atomic positions, respectively. No satellite reflections were observed on the diffraction images. The Ag and Cu atoms were refined isotropically and the site occupancy factors of the atomic positions were fixed at the last stage of the least-squares refinement. The increase of the disorder is most probably related to the difference in the covalent radii: $r(Na^+)$ = 1.86 Å, $r(Ag^+)$ = 1.44 Å and $r(Cu^+)$ = 1.28 Å,[29] and coordination number: CN(Na) = 5 and 6 (in compound **1**) and CN(Ag,

Cu) = 3 and 4 (in compounds **2** and **3)** of the cations. In the crystal structure of **2** and **3**, the Ag and Cu atoms possess distorted trigonal and tetrahedral coordination by sulfur atoms. The average Ag-S and Cu-S interatomic distances in **2** and **3** are *d*(Ag–S) = 2.85 Å and *d*(Cu–S) = 2.57 Å, respectively.

Ion-Exchange Property

It is well known that the porous crystalline materials, such as zeolites, containing negatively charged frameworks possess cation exchange property.[36] In analogy to zeolite materials, the crystal structure of **1** comprises large 6, 8, and 20 membered negatively charged channels and voids hosting the charge-balancing extra-framework Na cations. Therefore, the ion-exchange property of $Na(AlS_2)(GeS_2)_4$ (**1**) was thoroughly examined using different mono- and divalent metal salts.

$Na(AlS_2)(GeS_2)_4$ (**1**) exhibits facial ion-exchange capacity in DMF and some other solvents at room temperature with monovalent Ag^+ and Cu^+ cations. The processes have been done by adding a crystalline sample of the parent compound $Na(AlS_2)(GeS_2)_4$ (**1**) to a solution containing an equivalent amount of Ag or Cu cations yielding pure ion-exchanged products. The completeness of the cationic exchange process was confirmed by the single crystal X-ray diffraction, EDX, and ^{23}Na NMR spectroscopy. In most cases, the ion-exchange reactions require an excess amount of the exchange cation salts to form concentrated solutions.[20, 25] Here, we optimized the conditions where only 1:1 equivalent of **1** and Ag^+ or Cu^+ salts are required to produce pure phases of $Ag(AlS_2)(GeS_2)_4$ (**2**) and $Cu(AlS_2)(GeS_2)_4$ (**3**), respectively. Similar behavior was observed for the ion-exchange reaction of $(NH_4)_4In_{12}Se_{20}$ with heavy-metal ions (like Ag^+, Hg^{2+}, and Pb^{2+}), where exactly one equivalent of Ag or 0.5 equivalent of Hg or Pb was employed to yield almost pure ion-exchanged compounds.[37] Figure 3 displays the optical images of the compounds **1**-**3**. $Na(AlS_2)(GeS_2)_4$ (**1**) did not show any ion-exchange when treated with divalent transition metal salts such as $NiCl_2$, $Pd(CH_3COO)_2$, $Zn(CH_3COO)_2$ and $ZnCl_2$. This experimental evidence indicates that the $Na(AlS_2)(GeS_2)_4$ (**1**) possess preferred ion-exchange toward monovalent transition metal cations. In contrast, $K_2Sb_2Sn_3S_{10}$ was reported to have ion-exchange selectivity toward divalent metals such as Sr^{2+}, Cd^{2+} and Pb^{2+}.[19] Interestingly, $Ag(AlS_2)(GeS_2)_4$ (**2**) can also be obtained by an ion-exchange reaction of $Cu(AlS_2)(GeS_2)_4$ (**3**) with Ag^+ salt. However, $Ag(AlS_2)(GeS_2)_4$ (**2**) doesn't undergo ion-exchange when treated with Cu^+ salt, which shows the higher thermodynamical stability of the Ag analog compared to the Cu one, under the given condition. It is worth mentioning that compounds **2** and **3** were not accessible by direct combination reactions at elevated temperatures.

Spectroscopic Analysis

The solid-state ^{27}Al NMR spectra of compounds **1**, **2** and **3** recorded at room temperature under 14 kHz spinning rate are shown in Figure 4. The strong peaks observed between 122–132 ppm (single peak) are in the same range with the reported values for the aluminum in tetrahedral site $Al_{(tetra)}$.[38-39] The weak

peaks at 14 ppm can be assigned to the octahedral resonance of aluminum $Al_{(octa)}$,[40] which is associated with the oxidation product α-Al_2O_3 formed during the samples preparation.[14, 41] As expected, there is a slight shifting of the Al peak positions due to the replacement of Na with Ag in **2** and Cu in **3** (changing of the physical interaction between Na, Ag and Cu with S). This observation confirms that the coordination around Al atoms didn't change, otherwise the shift would be more significant. Moreover, NMR is a powerful technique to study oxidation state of metal ions. For example, Cu^{2+} is a paramagnetic ion and in a sample containing Cu^{2+}, Al NMR will be undetected due to paramagnetic relaxation mechanism.[42-43] Detection of the Al-chemical shift in compound **3**, gives a solid proof for the existence of diamagnetic Cu species (Cu^{+}) in **3**.[44]

The ^{23}Na NMR spectra of compounds **1**, **2** and **3** recorded under the same conditions are shown in Figure 5. There are two overlapped peaks at -15.96 ppm and -9.55 ppm for compound **1,** while no signals were observed for compounds **2** and **3**. This clearly proves the complete replacement of Na ions by Ag in compound **2** and Cu in compound **3**. The two overlapped peaks in compound **1** spectrum corresponds to the Na atoms with two different coordination, Na1 and Na2 (Figure 2d). Table 2 summarizes the observed Al and Na chemical shifts in compounds **1**-**3**.

The Raman spectra of compounds **1**-**3** are shown in Figure 6. The spectra show similar characteristic features related to GeS_4 tetrahedra in T_d point group symmetry. The sharp peak at 340 cm^{-1} corresponds to the Ge–S–Ge stretching mode, which falls in the same range of the ones found in *A*AlGeS_4 (*A* = Na, K),[14] and some alkali-metal thiogermanate glasses.[44] The weak peak at 171 cm^{-1} can be assigned to G–S bending mode referring to the Raman spectrum of $CsGe_4S_{10} \cdot 3H_2O$.[45] The bands at 362 and 431 cm^{-1} are corresponding to the terminal Ge-S stretching vibrations, which are very close to the ones found in Na_2GeS_3 and $Na_4Ge_4S_{10}$.[46] The peaks around 408 cm^{-1} and 132 cm^{-1} are comparable to the asymmetric vibrational modes observed in *A*AlGeS_4 (*A* = Na, K),[14] $A_4Ge_4S_{10}$ (*A* = K, Rb, Cs)[44], and $C_{14}NH_3GeS$.[47]

The UV-Vis. absorption spectra for all compounds were derived from diffuse reflectance data using the Kubelka-Munk function F(R).[48] Figure 7 shows the well-defined spectra of the compounds **1** and **3** with bandgap of 3.1 eV and 2.1 eV, respectively. The replacement of Na atoms in **1** with Cu resulted in 1 eV red-shift with a well-defined spectral response and negligible band-tailing.[49-50] In contrast, compound **2** exhibits an extended spectral response with a narrow bandgap of 1 eV (Figure 8). The wide range absorption behavior of this compound may originate from mid-gap states or result from compositional disorder within the structure due to the mobility of Ag ions.[51-53]

Thermal Analysis

The thermal stabilities of compounds **1**, **2** and **3** were examined by TG-DSC analysis up to 800 °C (Figure S4 (SI)). All three compounds are thermally stable up to 650 °C. Between 650 °C to 800 °C rather large weight losses were observed: 75 % for **1**, 35 % for **2** and 40 % for **3**. The samples were melted after the thermal analyses. The powder XRD pattern of **1** after the TG-DSC didn't reveal

presence of any crystalline residue, whereas peaks related to Ag_2GeS_3[54] and Cu_8GeS_6[55] were observed in case of **2** and **3**, respectively (Figure S5 (SI)). The thermal stability of the compounds **1**-**3** seems to be rather complicated and requires further detailed analyses.

Conclusions

The new member of the thioaluminogermanate family, $Na(AlS_2)(GeS_2)_4$ (**1**) was synthesized by a solid-state reaction. It possess a unique ion-exchange property in solvent media, at room temperature, toward Ag^+ and Cu^+, resulting in the isostructural $Ag(AlS_2)(GeS_2)_4$ (**2**) and $Cu(AlS_2)(GeS_2)_4$ (**3**) compounds, respectively. The crystal structure of **1**-**3** is composed of edge/corner-shared $(Al/Ge)S_4$ tetrahedra forming $[(AlS_2)(GeS_2)_4]^{1-}$ 3D polyanionic framework charge balanced by the *M* (*M* = Na, Ag, Cu) cations. The cation exchange study reveals further improvements of the parent compound (**1**) properties such as chemical stability; compound **1** is slightly air-sensitive while compounds **2** and **3** are air-stable. Also, it can lead to interesting properties, for example, the impact on the optical property; the 3.3 eV (wide bandgap) of **1** has been shifted to 2.3 eV after exchanging to **3** and furthermore, to a narrow band gap of 1eV after exchanging to **2**. The solid state ^{27}Al NMR proved the tetrahedral coordination of Al atoms in the crystal structure of **1**-**3** and therefore the rigidity of the anionic partial structure. The absence of any signal in the ^{23}Na NMR spectra of compounds **2** and **3** unambiguously demonstrate the completeness of the cation exchange processes.

Based on the initial findings, we propose a general formula of $(M_x)^{y+}((AlS_2)_y)^{y-}(GeS_2)_z\,(z \geq y)$ where *M* can be alkali, alkaline earth or transition metal, for designing new metal thioaluminogermanate compounds with intriguing chemical and physical properties.

Acknowledgements

This work was supported by the King Abdullah University of Science and Technology (KAUST) baseline fund BAS/1/1302–01–01.

References

1. Iyer, R. G.; Aitken, J. A.; Kanatzidis, M. G., Noncentrosymmetric cubic thio- and selenogermanates: $A_{0.5}M_{1.75}GeQ_4$ (A = Ag, Cu, Na; M = Pb, Eu; Q = S, Se). *Solid State Sci.* **2004,** *6*, 451-459.
2. Wu, X. W.; Hu, Y.; Pan, H.; Su, Z., $Na_9Sb(Ge_2Q_6)_2$ (Q = S, Se): two new antimony(III) quaternary chalcogenides with ethane-like $[Ge_2Q_6]^{6-}$ ligands. *RSC Adv.* **2016,** *6*, 99475-99481.
3. Choudhury, A.; Dorhout, P. K., Alkali-Metal Thiogermanates: Sodium Channels and Variations on the La_3CuSiS_7 Structure Type. *Inorg. Chem.* **2015,** *54*, 1055-1065.
4. Nakamura, Y.; Nakai, I.; Nagashima, K., Preparation and characterization of the new quaternary chalcogenides Tl-III-IV-S_4 (III = Al, Ga, In; IV = Si, Ge). *Mater. Res. Bull.* **1984,** *19*, 563-570.
5. Dong, Y.; Do, J.; Yun, H., Synthesis and Crystal Structures of the First Quaternary Tantalum Thiogermanates, $ATaGeS_5$ (A = K, Rb, Cs). *Z. Anorg. Allg. Chem.* **2009,** *635*, 2676-2681.
6. Liu, B.-W.; Zhang, M.-Y.; Jiang, X.-M.; Li, S.-F.; Zeng, H.-Y.; Wang, G.-Q.; Fan, Y.-H.; Su, Y.-F.; Li, C.; Guo, G.-C.; Huang, J.-S., Large Second-Harmonic Generation Responses Achieved by

the Dimeric $[Ge_2Se4(\mu\text{-}Se_2)]^{4-}$ Functional Motif in Polar Polyselenides $A_4Ge_4Se_{12}$ (A = Rb, Cs). *Chem. Mater.* **2017,** *29*, 9200-9207.
7. Marking, G. A.; Kanatzidis, M. G., The ethane-like $[Ge_2S_6]$ metals in $Na_8Pb_2[Ge_2S_6]_2$, $Na_8Sn_2[Ge_2S_6]_2$, and $Na_8Pb_2[Si_2Se_6]_2$. *J. Alloys Compd.* **1997,** *259*, 122-128.
8. Palchik, O.; Marking, G. M.; Kanatzidis, M. G., Exploratory Synthesis in Molten Salts: Role of Flux Basicity in the Stabilization of the Complex Thiogermanates $Cs_4Pb_4Ge_5S_{16}$, $K_2PbGe_2S_6$, and $K_4Sn_3Ge_3S_{14}$. *Inorg. Chem.* **2005,** *44*, 4151-4153.
9. Isaenko, L. I.; Yelisseyev, A. P.; Lobanov, S. I.; Krinitsin, P. G.; Molokeev, M. S., Structure and optical properties of $Li_2Ga_2GeS_6$ nonlinear crystal. *Opt. Mater.* **2015,** *47*, 413-419.
10. Tsuji, I.; Shimodaira, Y.; Kato, H.; Kobayashi, H.; Kudo, A., Novel Stannite-type Complex Sulfide Photocatalysts AI_2-Zn-AIV-S_4 (AI = Cu and Ag; AIV = Sn and Ge) for Hydrogen Evolution under Visible-Light Irradiation. *Chem. Mater.* **2010,** *22*, 1402-1409.
11. Davaasuren, B.; Emwas, A.-H.; Rothenberger, A., MAu_2GeS_4-Chalcogel (M = Co, Ni): Heterogeneous Intra- and Intermolecular Hydroamination Catalysts. *Inorg. Chem.* **2017,** *56*, 9609-9616.
12. Rothenberger, A.; Shafaei-Fallah, M.; Kanatzidis, M. G., Aluminosilicate Relatives: Chalcogenoaluminogermanates $Rb_3(AlQ_2)_3(GeQ_2)_7$ (Q = S, Se). *Inorg. Chem.* **2010,** *49*, 9749-9751.
13. Shannon, R. D., Revised Effective Ionic Radii and Systematic Studies of Interatomic Distances in Halides and Chalcogenides. *Acta Crystallogr. Sect. A* **1976,** *32*, 751-767.
14. Al-Bloushi, M.; Davaasuren, B.; Emwas, A.-H.; Rothenberger, A., Synthesis and Characterization of the Quaternary Thio-aluminogermanates $A(AlS_2)(GeS_2)$ (A = Na, K). *Z. Anorg. Allg. Chem.* **2015,** *641*, 1352-1356.
15. Kanatzidis, M. G., Discovery-Synthesis, Design, and Prediction of Chalcogenide Phases. *Inorg. Chem.* **2017,** *56*, 3158-3173.
16. Klein Haneveld, A. J.; Jellinek, F., Zirconium Silicide and Germanide Chalcogenides Preparation and Crystal Structures. *Recl. Trav. Chim. Pays-Bas* **1964,** *83*, 776-783.
17. Johrendt, D.; Tampier, M., $PdGeS_3$—A Novel One-Dimensional Metathiogermanate. *Chem. Eur. J.* **1998,** *4*, 1829-1833.
18. Sheldrick, W. S.; Wachhold, M., Solventothermal Synthesis of Solid-State Chalcogenidometalates. *Angew. Chem. Int. Ed.* **1997,** *36*, 206-224.
19. Yohannan, J. P.; Vidyasagar, K., Syntheses and Characterization of One-Dimensional Alkali Metal Antimony(III) Thiostannates(IV), $A_2Sb_2Sn_3S_{10}$ (A = K, Rb, Cs). *J. Solid State Chem.* **2015,** *221*, 426-432.
20. Yohannan, J. P.; Vidyasagar, K., Syntheses, Structural Variants and Characterization of $AInM'S_4$ (A = alkali metals, Tl; M′ = Ge, Sn) Compounds; Facile Ion-Exchange Reactions of Layered $NaInSnS_4$ and $KInSnS_4$ Compounds. *J. Solid State Chem.* **2016,** *238*, 291-302.
21. Qi, X. H.; Du, K. Z.; Feng, M. L.; Gao, Y. J.; Huang, X. Y.; Kanatzidis, M. G., Layered $A_2Sn_3S_7 \cdot 1.25H_2O$ (A = Organic Cation) as Efficient Ion Exchanger for Rare Earth Element Recovery. *J. Am. Chem. Soc.* **2017,** *139*, 4314-4317.
22. Manos, M. J.; Kanatzidis, M. G., Metal Sulfide Ion Exchangers: Superior Sorbents for the Capture of Toxic and Nuclear Waste-Related Metal Ions. *Chem. Sci.* **2016,** *7*, 4804-4824.
23. Chen, X.; Bu, X.; Lin, Q.; Mao, C.; Zhai, Q.-G.; Wang, Y.; Feng, P., Selective Ion Exchange and Photocatalysis by Zeolite-Like Semiconducting Chalcogenide. *Chem. Eur. J.* **2017,** *23*, 11913-11919.
24. Chen, S. H.; Yin, H. Q.; Zeng, D. M.; Chen, L. M., Synthesis of Flower-Like $Bi_2S_3/Cu_{7.2}S_4$ Composites and their Photocatalytic Performance. *Cryst. Res. Technol.* **2017,** *52*, 9.
25. Yang, H. J.; Luo, M.; Luo, L.; Wang, H. X.; Hu, D. D.; Lin, J.; Wang, X.; Wang, Y. L.; Wang, S.; Bu, X. H.; Feng, P. Y.; Wu, T., Highly Selective and Rapid Uptake of Radionuclide Cesium Based on Robust Zeolitic Chalcogenide via Stepwise Ion-Exchange Strategy. *Chem. Mater.* **2016,** *28*, 8774-8780.
26. Klemm, W.; Sodomann, H.; Langmesser, P., Beiträge Zur Kenntnis der Alkalimetallchalkogenide. *Z. Anorg. Allg. Chem.* **1939,** *241*, 281-304.
27. *X-Area IPDS software, STOE & Cie., Darmstadt*, STOE's Area Detector Software, STOE & Cie., Darmstadt: 2006.
28. *X-Shape Crystal Optimisation for Numerical Absorption Correction, STOE & Cie., Darmstadt*, Crystal Optimisation for Numerical Absorption Correction, STOE & Cie., Darmstadt: 1999.

29. Sheldrick, G., Crystal structure refinement with SHELXL. *Acta Crystallogr. Sect. C: Cryst. Struct. Commun.* **2015,** *71*, 3-8.
30. Putz, H.; Brandenburg, K., *Diamond - Crystal and Molecular Structure Visualization*, *Diamond 4*, Crystal Impact GbR, Bonn, Germany: 2015.
31. Eisenmann, B.; Hofmann, A., Crystal Structure of Hexasodium di-μ-thio-bis(dithioaluminate) – HT, $Na_6Al_2S_6$. *Z. Kristallogr.* **1991,** *197*, 161-162.
32. Wu, Y.; Nather, C.; Bensch, W., $Cs_4Ge_2S_8$. *Acta Crystallogr. Sect. Sect. E.* **2003,** *59*, i137-i138.
33. Klepp, K. O.; Zeitlinger, M., Crystal Structure of Tetracesium Decasulfidotetragermanate, $Cs_4Ge_4S_{10}$. *Z. Kristallogr. NCS.* **2000,** *215*, 7-8.
34. Klepp, K. O.; Fabian, F., New Chalcogenogermanates with Adamantane Type Complex Anions: Preparation and Crystal Structures of $K_4Ge_4S_{10}$; $Rb_4Ge_4S_{10}$, $Rb_4Ge_4Se_{10}$, and $Cs_4Ge_4Se_{10}$. *Z. Naturforsch. B* **1999,** *54*, 1499-1504.
35. Kuhn, A.; Eger, R.; Nuss, J.; Lotsch, B. V., Synthesis and Crystal Structures of the Alkali Aluminium Thiohypodiphosphates $MIAlP_2S_6$ (M = Li, Na). *Z. Anorg. Allg. Chem.* **2013,** *639*, 1087-1089.
36. Zheng, N.; Bu, X.; Feng, P., Synthetic Design of Crystalline Inorganic Chalcogenides Exhibiting Fast-Ion Conductivity. *Nat.* **2003,** *426*, 428-432.
37. Manos, M. J.; Malliakas, C. D.; Kanatzidis, M. G., Heavy-Metal-Ion Capture, Ion-Exchange, and Exceptional Acid Stability of the Open-Framework Chalcogenide $(NH_4)_4In_{12}Se_{20}$. *Chem. Eur. J.* **2007,** *13*, 51-58.
38. Skibsted, J.; Jakobsen, H. J.; Hall, C., Direct Observation of Aluminium Guest Ions in the Silicate Phases of Cement Minerals by ^{27}Al MAS NMR Spectroscopy. *J. Chem. Soc. Faraday Trans.* **1994,** *90*, 2095-2098.
39. Jackson, M. D.; Chae, S. R.; Mulcahy, S. R.; Meral, C.; Taylor, R.; Li, P.; Emwas, A.-H.; Moon, J.; Yoon, S.; Vola, G.; Wenk, H.-R.; Monteiro, P. J. M., Unlocking the Secrets of Al-tobermorite in Roman Seawater Concrete. *Am. Mineral*. **2013,** *98*, 1669-1687.
40. Kapoor, P. N.; Heroux, D.; Mulukutla, R. S.; Zaikovskii, V.; Klabunde, K. J., High Surface Area Homogeneous Nanocrystalline Bimetallic Oxides Obtained by Hydrolysis of Bimetallic [Small Micro]-oxo Alkoxides. *J. Mater. Chem.* **2003,** *13*, 410-414.
41. Woo, A. J., Single-Crystal ^{27}Al NMR Study of Corundum *a*-Al_2O_3. *Bull. Korean Chem. Soc.* **1999,** *20*, 1205-1208.
42. Emwas, A. H. M.; Al-Talla, Z. A.; Guo, X. R.; Al-Ghamdi, S.; Al-Masri, H. T., Utilizing NMR and EPR Spectroscopy to Probe the Role of Copper in Prion Diseases. *Magn. Reson. Chem.* **2013,** *51*, 255-268.
43. Blindauer, C. A.; Emwas, A. H.; Holy, A.; Dvorakova, H.; Sletten, E.; Sigel, H., Complex Formation of the Antiviral 9- 2-(Phosphonomethoxy)Ethyl Adenine (PMEA) and of its N1, N3, and N7 Deaza Derivatives with Copper(II) in Aqueous Solution. *Chem. Eur. J.* **1997,** *3*, 1526-1536.
44. Nelson, C. R.; Poling, S. A.; Martin, S. W., Synthesis and Characterization of Potassium, Rubidium, and Cesium Thiogermanate Glasses. *J. Non-Cryst. Solids* **2004,** *337*, 78-85.
45. Pohl, S.; Krebs, B., Darstellung und Struktur von $Cs_4Ge_4S_{10} \cdot 3H_2O$. *Z. Anorg. Allg. Chem.* **1976,** *424*, 265-272.
46. Barrau, B.; Ribes, M.; Maurin, M.; Kone, A.; Souquet, J.-L., Glass Formation, Structure and Ionic Conduction in the $Na_2S.GeS_2$ System. *J. Non-Cryst. Solids* **1980,** *37*, 1-14.
47. Rangan, K. K.; Kanatzidis, M. G., Mesolamellar Thiogermanates $[C_nH_{2n+1}NH_3]_4Ge_4S_{10}$. *Inorg. Chim. Acta* **2004,** *357*, 4036-4044.
48. Kortüm, G., *Reflectance Spectroscopy, Principles, Methods, Applications*. Springer-Verlag Berlin Heidelberg: 1969.
49. Mansour, B.; El Akkad, F.; Hendeya, T., Electrical and Thermoelectric Properties of Some Copper Chalcogenides. *Phys. Status Solidi A.* **1980,** *62*, 495-501.
50. Yang, H.; Wang, L.; Hu, D.; Lin, J.; Luo, L.; Wang, H.; Wu, T., A Novel Copper-Rich Open-Framework Chalcogenide Constructed from Octahedral Cu_4Se_6 and Icosahedral Cu_8Se_{13} Nanoclusters. *Chem. Commun.* **2016,** *52*, 4140-4143.
51. Kim, T. W.; Garrod, T. J.; Kim, K.; Lee, J. J.; LaLumondiere, S. D.; Sin, Y.; Lotshaw, W. T.; Moss, S. C.; Kuech, T. F.; Tatavarti, R.; Mawst, L. J., Narrow Band Gap (1 eV) InGaAsSbN Solar Cells Grown by Metalorganic Vapor Phase Epitaxy. *Appl. Phys. Lett.* **2012,** *100*, 121120.

52. Nelson, H. D.; Hinterding, S. O. M.; Fainblat, R.; Creutz, S. E.; Li, X.; Gamelin, D. R., Mid-Gap States and Normal vs Inverted Bonding in Luminescent Cu^{+}- and Ag^{+}-Doped CdSe Nanocrystals. *J. Am. Chem. Soc.* **2017,** *139*, 6411-6421.
53. Tansho, M.; Wada, H.; Ishii, M.; Onoda, Y., Mobility of Silver Ions in Silver Ion Conductor Ag_7NbS_6 Studied by Ag and Nb NMR. *J. Phys. Chem. B* **1998,** *102*, 5047-5049.
54. Nagel, A.; Range, K. J., Compound Formation in System Ag_2S-GeS_2-AgI. *Z. Naturforsch. B* **1978,** *33*, 1461-1464.
55. Ishii, M.; Onoda, M.; Shibata, K., Structure and Vibrational Spectra of Argyrodite Family Compounds Cu_8SiX_6 (X = S, Se) and Cu_8GeS_6. *Solid State Ion.* **1999,** *121*, 11-18.

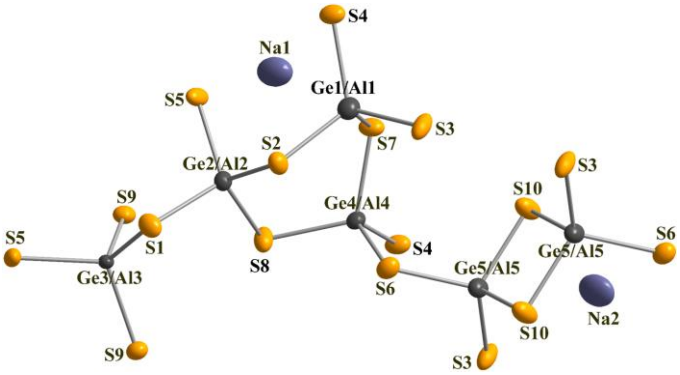

Figure 1. A projection of the 3D structure showing the atomic distribution and connectivity of $Na(AlS_2)(GeS_2)_4$ (**1**) .

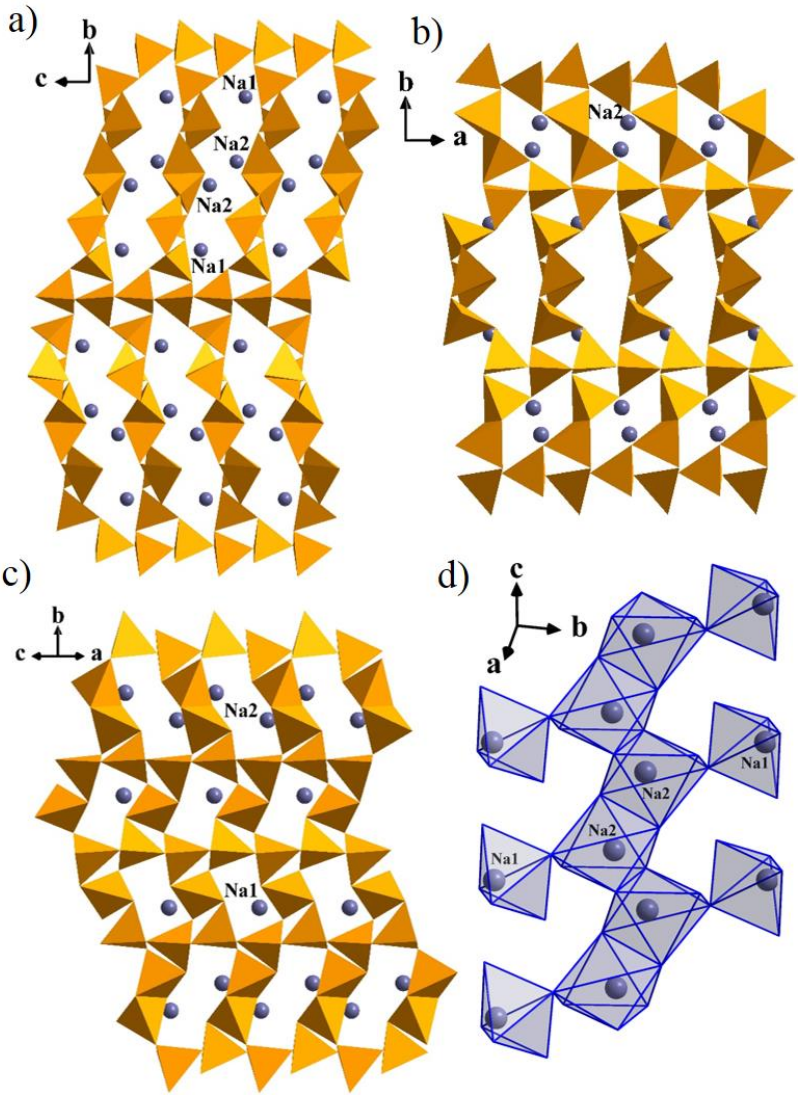

Figure 2. Crystal structure of $Na(AlS_2)(GeS_2)_4$ (**1**): a) A projection of the 3D framework along *a* axis, Na1 and Na2 occupying the voids with the length of 2.6 nm, b) A projection of the 3D framework along *c* axis, only Na2 occupies parallelogram voids, c) A projection of the 3D framework along the [101], Na1 and Na2 occupying different voids, d) The connectivity of the $(Na2)S_6$ octahedral chains with isolated $(Na1)S_5$ bipyramidal units. The yellow tetrahedra represent $(Al/Ge)S_4$.

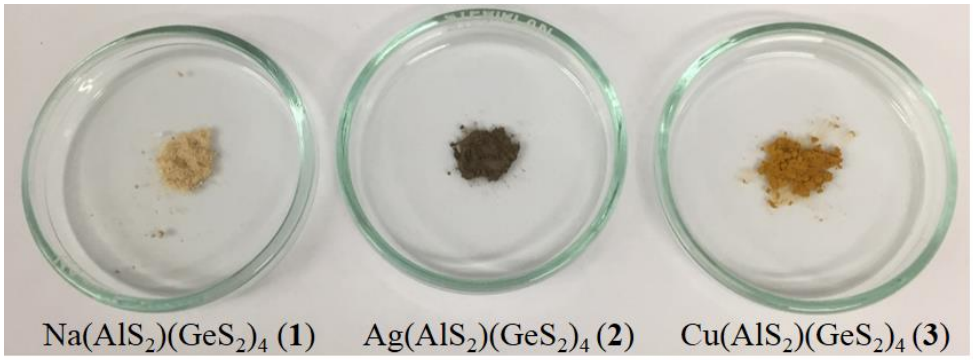

Figure 3. The optical image of the parent compound $Na(AlS_2)(GeS_2)_4$ (**1**) and the exchanged compounds $Ag(AlS_2)(GeS_2)_4$ (**2**) and $Cu(AlS_2)(GeS_2)_4$ (**3**).

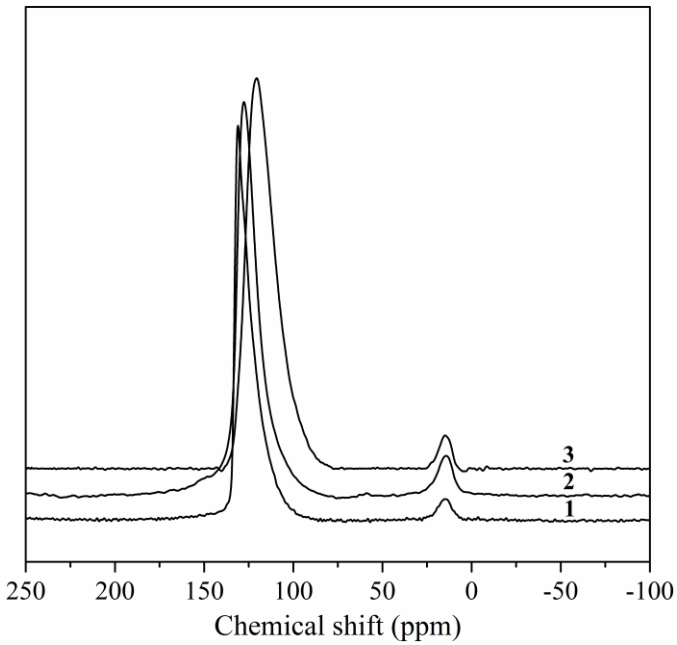

Figure 4. ^{27}Al NMR spectra of $Na(AlS_2)(GeS_2)_4$ (**1**), $Ag(AlS_2)(GeS_2)_4$ (**2**) and $Cu(AlS_2)(GeS_2)_4$ (**3**) recorded at 14 kHz spinning rate.

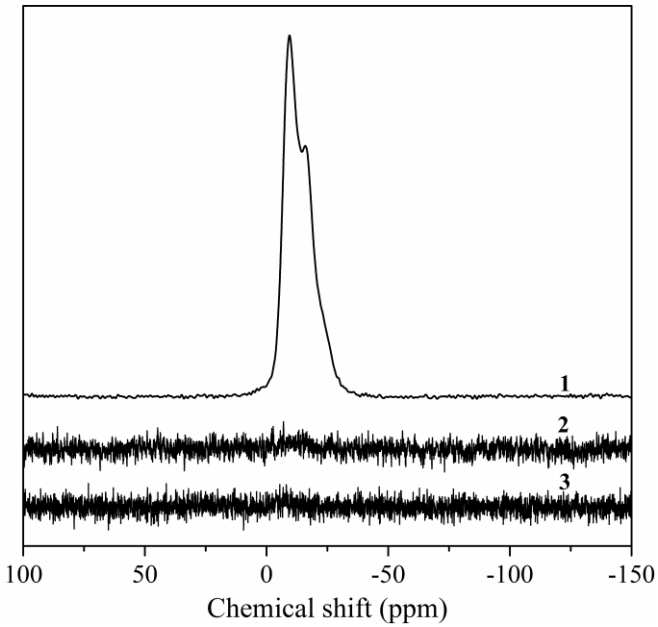

Figure 5. ^{23}Na NMR spectra of $Na(AlS_2)(GeS_2)_4$ (**1**), $Ag(AlS_2)(GeS_2)_4$ (**2**) and $Cu(AlS_2)(GeS_2)_4$ (**3**) recorded at 14 kHz spinning rate.

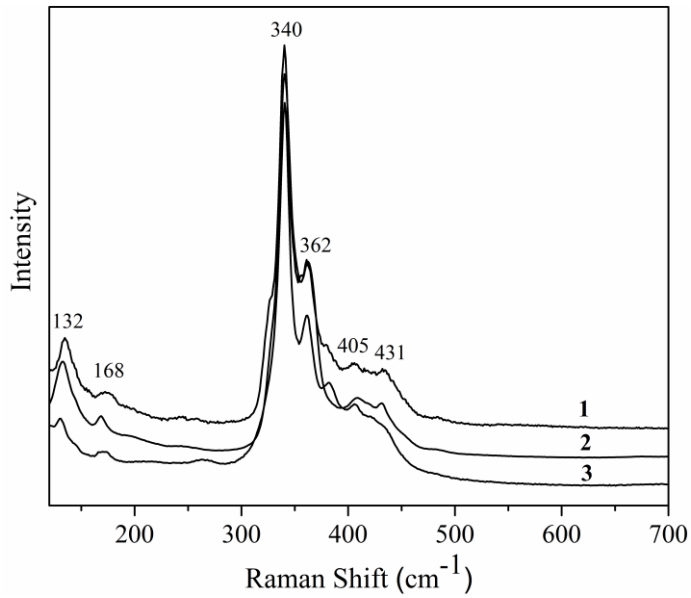

Figure 6. Raman spectra of $Na(AlS_2)(GeS_2)_4$ (**1**), $Ag(AlS_2)(GeS_2)_4$ (**2**) and $Cu(AlS_2)(GeS_2)_4$ (**3**).

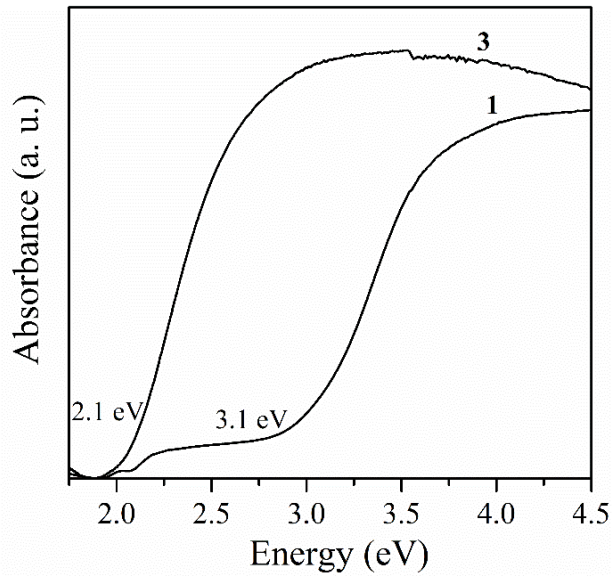

Figure 7. UV/Vis absorption spectra of $Na(AlS_2)(GeS_2)_4$ (**1**) and $Cu(AlS_2)(GeS_2)_4$ (**3**).

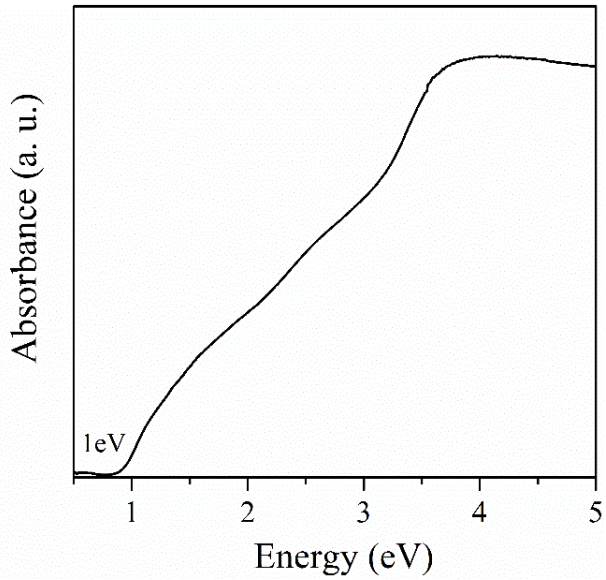

Figure 8. UV/Vis absorption spectra of $Ag(AlS_2)(GeS_2)_4$ (**2**).

Table 1. Crystallographic data and details on data collection and structure refinement for compounds **1**–**3**.

Compound	**1**	**2**	**3**
Formula	$NaAlGe_4S_{10}$	$AgAlGe_4S_{10}$	$CuAlGe_4S_{10}$
Formula weight	660.93	745.81	701.48
T /K	200(2)	200(2)	150(2)
Crystal system	Monoclinic	Monoclinic	Monoclinic
Space group	$P2_1/n$ (14)	$P2_1/n$ (14)	$P2_1/c$ (14)
a /Å	6.803(3)	6.798 (1)	6.796(1)
b /Å	38.207(2)	38.416(8)	37.628(8)
c /Å	6.947(4)	6.812(1)	6.879(1)
α /°	90	90	90
β /°	119.17(3)	119.65(3)	119.52(3)
γ /°	90	90	90
V /Å^3	1576.91(1)	1546.4(7)	1530.9(7)
Z	4	4	4
ρ /g·cm^{-3}	2.784	3.204	3.044
μ /mm^{-1}	2.784	10.303	10.516
F(000)	1248	1392	1320
Reflections collected	14193	19025	13978
Unique data	4149	4186	4136
R_{int}	0.0722	0.0731	0.0314
Parameters	155	157	160
R_1 [$I > 2\sigma(I)$]	0.0566	0.0569	0.0512
wR_2 (all data)	0.1814	0.1539	0.1429

Further details of the crystal structure investigation may be obtained from Fachinformationszentrum Karlsruhe, 76344 Eggenstein- Leopoldshafen, Germany (Fax: (+49)7247-808-666; E-mail: crysdata(at)fiz-karlsruhe(dot)de, http://www.fiz-karlsruhe.de/request_ for_deposited_data.html) on quoting the depository CSD numbers of 433748 for **1**, 433750 for **2** and 433749 for **3**.

Table 2. The $^{27}Al_{(tetra)}$ and ^{23}Na chemical shifts (δ) for compounds **1-3**

Compound	$Al_{(tetra)}$ δ ppm	Na δ ppm
1	131.10	-15.96 and -9.55
2	127.97	-
3	121.14	-

Entry for the Table of Contents

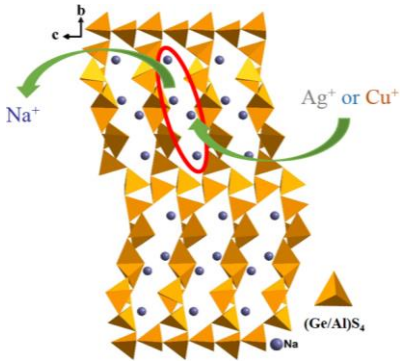

For Table of Contents Only

Synopsis

Zeolite-like thioaluminogermanate $Na(AlS_2)(GeS_2)_4$ exhibit a unique ion-exchange capability in solvent media, at room temperature, to completely replace the Na^+ with monovalent transition metals Ag^+ and Cu^+. The ion-exchange products possess higher air stability and narrower bandgap energies compared to the parent compound.